Yongming Bian, Xiaomei Liu, Anhu Li and Yongcheng Liang*

A Crossover from High Stiffness to High Hardness: The Case of Osmium and Its Borides

DOI 10.1515/zna-2016-0211
Received May 29, 2016; accepted July 3, 2016; previously published online July 26, 2016

Abstract: Transition-metal light-element compounds are currently raising great expectations for hard and superhard materials. Using the widely attracting osmium (Os) and its borides (OsB, Os_2B_3 and OsB_2) as prototypes, we demonstrate by first-principles calculations that heavy transition metals, which possess high stiffness but low hardness, can be converted into highly hard materials by incorporating of light elements to form compounds. Such a crossover is a manifestation that the underlying sources of high stiffness and high hardness are fundamentally different. The stiffness is related to elastic deformation that is closely associated with valence electron density, whereas the hardness depends strongly on plastic deformation that is determined by bonding nature. Therefore, the incorporation of light atoms into transition metal should be a valid pathway of designing hard and superhard materials. This strategy is in principle also applicable to other transition-metal borides, carbides, and nitrides.

Keywords: First-Principles Calculations; Mechanical Properties; Transition Metal Borides.

1 Introduction

Hard and superhard materials are technologically important in many applications from reducing the wear of everyday objects to creating machining tools [1, 2]. Experimentally, the hardness of a material is defined by pressing a diamond indenter into the surface of the material and measuring the size of the impression. It is obvious that the hardness definition is a macroscopic concept, which leads to the difficulty in calculating the hardness value microscopically; thus, theoretical scientists need to look for an additional replacement of hardness. A frequently used candidate for this is the bulk modulus, which reflects the volume stiffness of the material [3]. It is often true that a highly hard material must possess a high bulk modulus. For example, diamond is the hardest existing material with the highest known bulk modulus. However, it is a bit confusing whether a material with a high bulk modulus has a high hardness. In fact, bulk modulus has little direct connection with hardness. For example, the bulk modulus of WC is as high as 439 GPa but its hardness is below 30 GPa [4]. Nevertheless, B_6O possesses a higher hardness between 32 and 60 GPa even though its relatively lower bulk modulus of 230 GPa [5]. Therefore, it is highly desirable to hunt for a type of prototype materials to exemplify the exact difference of high stiffness and high hardness and, in particular, to provide the essential guidance in the design of hard and superhard materials.

In the last years, transition-metal Os has attracted much attention. Its bulk modulus was first measured to be 462 GPa by Cynn et al. [6] and later reported to be 411 GPa by Occelli et al. [7] and 395 GPa by Kenichi [8] using different experimental methods. These values are considered to be extremely high, exceeding that of cubic boron nitride (392 GPa) and even rivaling with that of diamond (446 GPa) [9]. Based on high bulk modulus, it has been proposed that incorporating light atoms (e.g. boron, carbon, and nitrogen) into heavy transition metals (e.g. Os, Re, and W) might be a possible strategy to design hard and superhard materials [10–12]. Theoretically, a series of transition-metal borides have been predicted for promising hard and superhard [13–17]. Implicit in such efforts is an assumption that the metal atoms (creating high valence-electron density) prevent the structures from being squeezed together, while the light atoms (forming strong covalent bond) withstands both elastic and plastic deformations, both of which enhance the hardness of materials. By applying this principle, the first prototype material OsB_2 was synthesised and was characterised to be an ultra-incompressible, hard material [11]. Subsequently, OsB and Os_2B_3 have also been synthesised experimentally [18]. So far, there are a few theoretical works reporting their mechanical properties and electronic structures [19–23],

***Corresponding author: Yongcheng Liang,** College of Engineering Science and Technology, Shanghai Ocean University, Shanghai 201306, China, Tel.: +86-21-61900820, Fax: +86-21-61900805, E-mail: ycliang@shou.edu.cn
Yongming Bian and Anhu Li: School of Mechanical Engineering, Tongji University, Shanghai 200092, China
Xiaomei Liu: School of Mechanical Engineering, Tongji University, Shanghai 200092, China; and College of Mechanical Engineering, Shanghai University of Engineering Science, Shanghai 200062, China

but these calculated results are quite scattered due to the inconsistency in different techniques. In particular, the changing trends of stiffness and hardness have not fully addressed.

In this article, we systematically investigate the equation of state (EOS), elastic properties, and hardness of Os, OsB, Os_2B_3, and OsB_2 using the first-principles calculations. The transition-metal Os has high stiffness but low hardness. While the incorporation of boron into the lattice structure of Os forms OsB, Os_2B_3, and OsB_2, their bulk moduli decrease steadily but their hardness values enhance rapidly. We reveal that the crossover from high stiffness to high hardness is a result of their completely different underlying origins, which may provide a new strategy of designing hard and superhard materials.

2 Structures and Methods

Experimentally, Os adopts the hexagonal close-packed (hcp) lattice (space group $P6_3/mmc$) [6–8]. OsB (space group $P\text{-}6m2$) and Os_2B_3 (space group $P6_3/mmc$) form in the hexagonal lattice with few freedoms of atomic positions as shown in Figure 1a and b, respectively. OsB has only one formula unit per unit cell with one Os atoms on the 1*a* (0, 0, 0) Wyckoff site and one B atom on the 1*d* (1/3, 2/3, 1/2) position [18]. For Os_2B_3, there are two formula units per unit cell, in which four Os atoms occupy the 4*f* (2/3, 1/3, 0.6398) sites and six B atoms hold the 2*d* (2/3, 1/3, 3/4) and 4*f* (2/3, 1/3, 0.4727) positions [18]. As shown in Figure 1c, OsB_2 crystallises the related body-centered orthorhombic structure with the space group of *Pmmn*. In each unit cell, two Os atoms are situated in the 2*a* (2/3, 1/3, 3/4) sites, whereas four B atoms occupy the 4*f* (2/3, 1/3, 0.455) positions [11, 18].

First-principles calculations based on density functional theory (DFT) have been performed for Os, OsB, Os_2B_3, and OsB_2 using the all-electron projector augmented wave (PAW) method within the generalised gradient approximation (GGA) of Perdew, Burke, and Ernzerhof (PBE) [24], as implemented in VASP code [25]. A very careful check for the convergence of calculated results with respect to the kinetic cutoff energy and the number of *k*-points has been conducted. We finally adopt a plane-wave basis set with a large cutoff energy of 500 eV and the *k*-mesh with a dense grid of 0.025 $Å^{-1}$ for all the considered systems to ensure the numerical accuracy.

We carry out total-energy calculations over a wide range of volumes for the considered materials. The structure optimisations are performed for each constant volume and each material. The equilibrium volume, bulk modulus, and its first pressure derivative are estimated through a least-square fit of calculated volume-energy sets to the third-order Birch–Murnaghan EOS [26]. The elastic constants are obtained by the efficient strain energy method with the maximum strain of 0.04, and the details

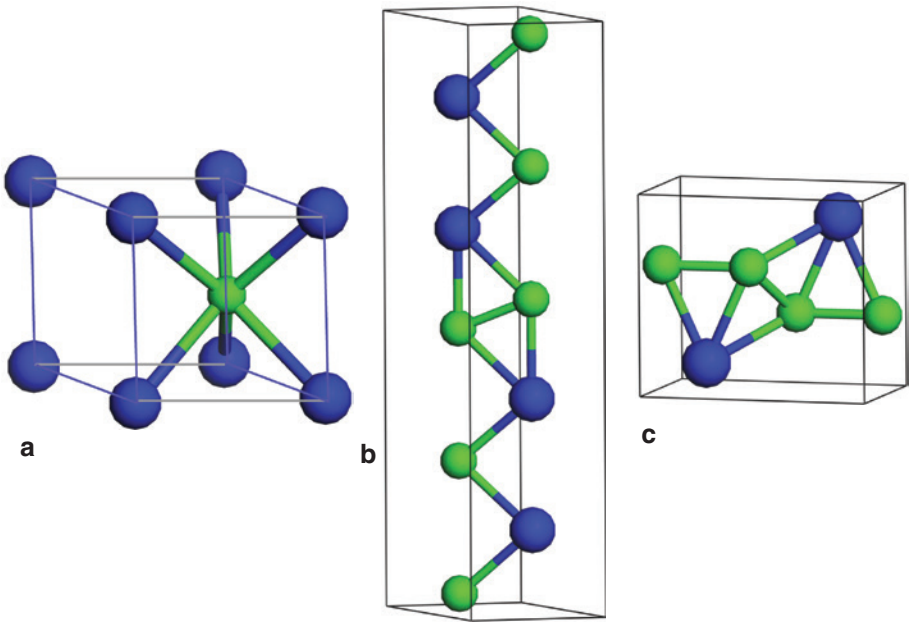

Figure 1: Crystal structures of the (a) hexagonal OsB, (b) hexagonal Os_2B_3, and (c) orthorhombic OsB_2. The blue (large) and green (small) spheres represent Os and B atoms, respectively.

are described in our previous work [22]. This method has been demonstrated to be very good in providing accurate and reliable predictions of mechanical properties of various systems [27–29]. According to the Voight–Reuss–Hill bounds [30], their shear moduli, Young's moduli, and Poisson's ratio are also determined. For diamond, OsB, Os_2B_3, and OsB_2, the Vickers' hardness values are estimated by Chen's model [31].

3 Results and Discussion

Table 1 lists the space group, calculated equilibrium lattice constants, equilibrium volume, bulk modulus, its pressure derivative at zero pressure with available data for Os, OsB, Os_2B_3, and OsB_2. For comparison, diamond has also been studied in this work. From this table, we can see that these calculated results are in relatively good agreement with the experimental data within the GGA errors, and this confirms the validity of our calculations. As expected, diamond has the highest known bulk modulus (433 GPa) among the five materials. For the transition-metal Os, its bulk modulus is predicted to be 404 GPa, which agrees well with the experimental measurements [6–8]. This value is slightly smaller than that of diamond, and thus, Os is an ultrastiff material. While boron atoms insert into Os to form its borides, the bulk modulus steadily decreases from 357 GPa for OsB to 334 GPa for Os_2B_3 and then to 311 GPa for OsB_2. To further compare the volume stiffness of diamond, Os, OsB, Os_2B_3, and OsB_2 under pressure, the volume compressions as a function of pressure are plotted in Figure 2. We can explicitly see that the order of volume stiffness from high to low is diamond > Os > OsB > Os_2B_3 > OsB_2, although they all have very high volume stiffness.

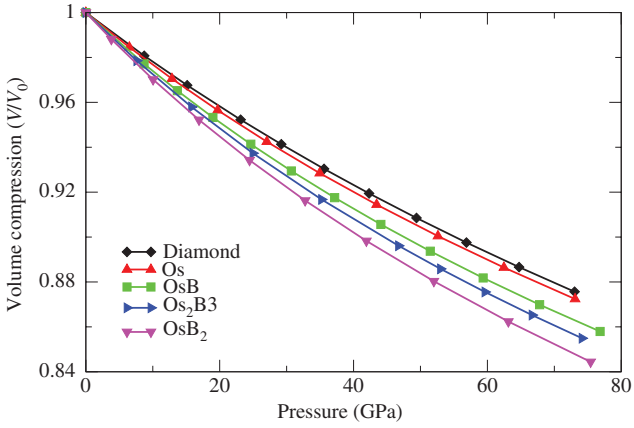

Figure 2: Calculated volume compression (V/V_0) under pressure for diamond, Os, OsB, Os_2B_3, and OsB_2.

The accurate calculation of elasticity is essential for understanding the macroscopic mechanical properties of solids, for establishing the constitutive equations and for the design of hard materials. Our obtained elastic constants, shear moduli, Young's moduli, and Poisson's ratios for diamond, Os, OsB, Os_2B_3, and OsB_2 are presented in Table 2. For the cubic, hexagonal, and orthorhombic lattices, there are three (C_{11}, C_{12}, and C_{44}), five (C_{11}, C_{12}, C_{13}, C_{33}, and C_{44}), and nine independent elastic constants (C_{11}, C_{12}, C_{13}, C_{22}, C_{23}, C_{33}, C_{44}, C_{55}, and C_{66}), respectively. First, the mechanical stability of any crystal complies with the mandatory requirement of the strain energy to be positive. We have carefully checked these calculated elastic constants C_{ij} and the results show that the five materials are mechanically stable at zero pressure. Then, the elastic constants C_{11}, C_{22}, or C_{33} measure the *a*-, *b*-, or *c*-direction resistance to linear compression, respectively. All three directions of diamond are isotropic and possess the highest linear

Table 1: Space group, equilibrium lattice constants a_0, b_0, c_0 (Å), equilibrium volume V_0 (Å^3), bulk modulus B_0 (GPa), and its pressure derivative B_0' at zero pressure compared with available data for diamond, Os, OsB, Os_2B_3, and OsB_2.

Materials	Space group	a_0	b_0	c_0	V_0	B_0	B_0'	
Diamond	*Fd*-3*m*	3.575	3.575	3.575	45.68	433	3.62	This study
		3.567	3.567	3.567	45.38	446	3.0	Expt. [9]
Os	$P6_3/mmc$	2.755	2.755	4.344	28.54	404	4.92	This study
		2.733	2.733	4.318	27.941	395–462	2.4–4.5	Expt. [6–8]
OsB	*P*-6*m*2	2.899	2.899	2.882	20.98	357	4.42	This study
		2.876	2.876	2.873	20.58	431	5.8	Expt. [18]
Os_2B_3	$P6_3/mmc$	2.943	2.943	12.943	97.08	334	4.41	This study
		2.909	2.909	12.945	94.88	396	7.1	Expt. [18]
OsB_2	*Pmmn*	4.705	2.890	4.093	55.66	311	4.24	This study
		4.684	2.871	4.075	54.80	343	4.4	Expt. [18, 19]

Table 2: Calculated elastic constants C_{ij} (GPa), shear modulus G (GPa), Young's modulus E (GPa), Poisson's ratio υ, and hardness H (GPa) for diamond, Os, OsB, Os_2B_3, and OsB_2.

Material	C_{11}	C_{22}	C_{33}	C_{12}	C_{13}	C_{23}	C_{44}	C_{55}	C_{66}	G	E	υ	H	H (Exp.)
Diamond	1049	1049	1049	127	127	127	573	573	573	525	1123	0.069	94.8	93.5[a]
Os	747	747	832	227	231	231	254	254	260	262	649	0.237	–	4[b]
OsB	635	635	809	201	200	200	193	193	217	217	543	0.250	20.0	14.4[b]
Os_2B_3	556	556	910	202	193	193	215	215	177	212	530	0.247	24.0	21.8[b]
OsB_2	588	578	846	184	222	121	163	286	215	225	552	0.226	29.6	23.5[b]

The theoretical hardness of Os is not estimated due to the failure of the hardness model to pure metallic compounds.

[a]Reference [21].

[b]Reference [18].

stiffness (1049 GPa). The linear stiffness of Os is inferior to that of diamond but is superior to that of OsB, Os_2B_3, and OsB_2. Moreover, we interestingly find that there is substantial anisotropy in the mechanical behavior of OsB, Os_2B_3, and OsB_2. It is observed that C_{11} for OsB (635 GPa), Os_2B_3 (556 GPa), and OsB_2 (588 GPa) are smaller by 39 %, 47 %, and 44 %, respectively, compared with that of diamond (1049 GPa). However, C_{33} for OsB (809 GPa), Os_2B_3 (910 GPa), and OsB_2 (846 GPa) are comparable to that of diamond. In addition, Young's moduli for OsB (543 GPa), Os_2B_3 (530 GPa), and OsB_2 (552 GPa) are only half of that of diamond (1123 GPa). It is obvious that the off-diagonal elastic constants and Possion's ratios for OsB, Os_2B_3, and OsB_2 are much larger than the corresponding values of diamond. We have further calculated the axial ratios c/a or c/b as function of pressure. As seen from Figure 3, OsB, Os_2B_3, and OsB_2 exhibit substantial anisotropy under high pressure. Therefore, the present results show that the linear stiffness of Os is superior to that of OsB, Os_2B_3, and OsB_2, although OsB, Os_2B_3, and OsB_2 also have high linear stiffness and anisotropy.

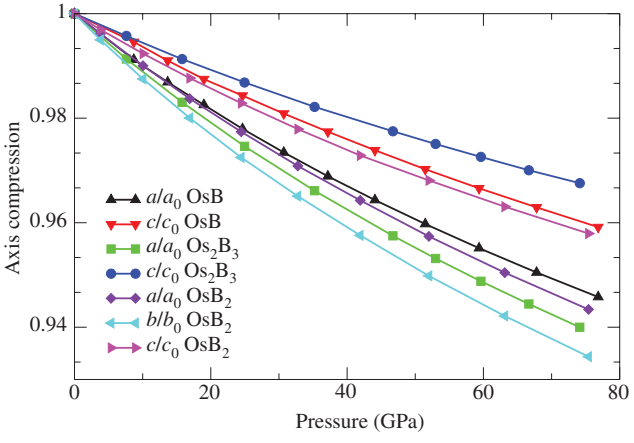

Figure 3: Calculated axis compression (a/a_0, b/b_0, and c/c_0) under pressure for OsB, Os_2B_3, and OsB_2.

Shear stiffness measures the resistance to shape change under the applied loads. The shear moduli of Os, OsB, Os_2B_3, and OsB_2 are calculated to be 262, 217, 212, and 225 GPa, respectively. Clearly, the shear stiffness of Os is superior to that of its borides (OsB, Os_2B_3, and OsB_2) but only approaches 50 % of that of diamond (525 GPa). The elastic constants C_{44}, C_{55}, and C_{66} are also an important parameter to describe the shear property of a material. For OsB, its C_{44} (193 GPa) is smaller than C_{66} (217 GPa); for Os_2B_3, C_{44} (215 GPa) is larger than C_{55} (177 GPa). For orthorhombic OsB_2, the elastic constants C_{44}, C_{55}, and C_{66} are calculated to be 163, 286, and 215 GPa, respectively. Therefore, these results indicate that the shear stiffness of OsB, Os_2B_3, and OsB_2 not only is inferior to that of Os but also exhibit substantial anisotropy.

The hardness values are presented in Table 2 for diamond, Os, OsB, Os_2B_3, and OsB_2. Except for Os, the estimated hardness values agree with the measured results. Below the experimental data are adopted to discuss their trend. We notice that the changing trend of hardness is completely different from that of stiffness. Although the bulk modulus of Os rivals with that of diamond, the hardness of Os (4 GPa) is by far smaller than that of diamond (93.5 GPa), implying that ultrastiff Os is not a hard material at all. Hence, high stiffness does not guarantee high hardness. Nevertheless, can a highly stiff material transform into a highly hard one? In diamond, the four sp^3 hybrids of carbon form a three-dimensional network composed of strong covalent bonds, which is responsible for its hardness. At the same time, its high valence electron density results in its exceptionally high bulk modulus. The high stiffness of Os can be explained from its high valence electron density, and its low hardness is attributed to the weak metallic bonds that allow plastic deformation. In order to enhance the hardness of a material, the nondirectional metallic bonds must be changed to directional covalent bonds by inserting light atoms into transition metals. With the addition of boron atoms, the values of hardness

enhance from 14.4 GPa for OsB to 21.8 GPa for Os_2B_3 and then to 23.5 GPa for OsB_2. These results demonstrate that the transition-metal Os, which has high stiffness but low hardness, is converted into hard materials by incorporating of boron atoms to form borides. Such a crossover is a manifestation that the underlying sources of high stiffness and high hardness are fundamentally different. Moreover, the opposite trends of stiffness and hardness for Os and its borides provide an illustrative case explicitly to differentiate their natures.

Upon incorporating boron atoms into the interstitial sites of the Os lattice to form OsB, the crystal volume largely expands. This volume expansion results in the drop in valence electron density and thus gives rise to a negative contribution to the bulk modulus. As shown in Figure 1a, the structure of OsB can be described as stacking of Os- and B-layers along the *c*-direction and the covalent bonds of Os-B are formed, which achieves the sharp hardness enhancement from Os to OsB. With the increasing in boron content, the valence electron density continues to fall slowly, and thus, the bulk modulus slightly decreases from OsB to Os_2B_3, then to OsB_2. However, for Os_2B_3, the boron atoms of puckered layers are tetrahedrally surrounded by four Os atoms and three additional boron neighbors. The boron atoms of planar layers have a trigonal prismatic environment of six Os atoms and no adjacent boron atoms (see Fig. 1b). The higher degree of covalent bonding makes the hardness of Os_2B_3 increase. In OsB_2, there exist well-defined zigzag covalent chains along the *c*-direction, interconnected by shared B and Os atoms. This feature of covalent bond network plays a key role in enhancing its hardness, but the presence of soft metallic Os–Os layers limits its enhanced hardness at a large load [21]; thus, OsB_2 is a hard but not superhard material. In order to understand the underlying origin of hardness enhancement, we use Os and OsB_2 as an illustrative case to compare their electronic structures. Our calculated density of states (DOS) for Os and OsB_2 are plotted in Figure 4. As can be seen, the electronic structure of Os is predominated by 5*d* states while that of OsB_2 is governed by a strong hybridisation between the Os-5*d* and B-2*p* states. It is the crossover from partially metallic bonds to covalent bonds that has an important contribution to the hardness enhancement from Os to its borides. Ideally, a boron-richer compound would be a preferred harder material, as a higher concentration of boron may easily lead to a three-dimensional B–B bonding and thus a higher hardness. Therefore, pursuing boron-rich borides has recently stimulated much interest and some transition-metal borides with high boron content, such as WB_3, FeB_4, and MnB_4 [32–34], have become the prime

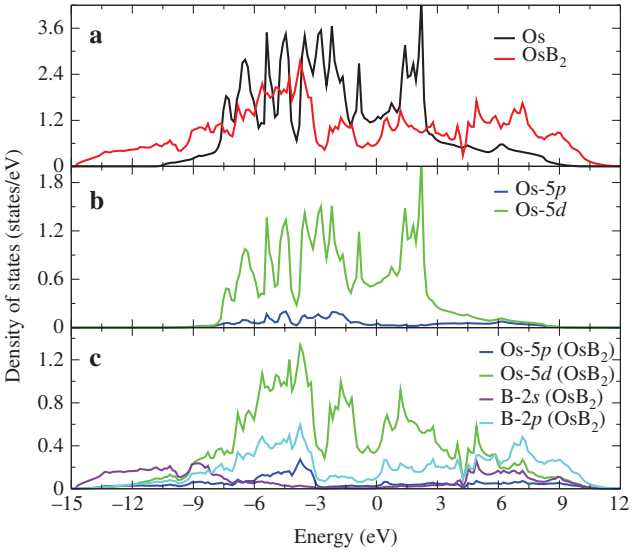

Figure 4: Density of states (DOS). (a) total DOS of Os and OsB_2, (b) projected DOS of Os, and (c) projected DOS of OsB_2.

candidates to be superhard materials. Pursuing the thermodynamically stable transition-metal borides with ultimate boron content may be a reasonable strategy used for designing hard and superhard materials [35].

Finally, we briefly discuss the relation between mechanical properties and deformations. In order to split a crystal, electron-pair covalent bonds must first be broken and remade. Accordingly, hardness depends strongly on plastic deformation that is mainly determined by bonding nature. However, bulk modulus measures resistance to elastic compression of volume, which has little direct connection with hardness from dislocation theory. In elastic deformation, the basic relations between atoms do not change. Therefore, valence electron density mostly determines the bulk modulus of a material, but the bonding nature, optimal filling of bonding states, and crystal structure also partially contribute to the stiffness. In general, covalent materials show high bond-bending force constants, contain highly directional bonds, and thus possess high shear modulus. Although a good correlation has been observed between hardness and shear modulus, the dependence is not unequivocal and monotonic [36]. Thus, it is sometimes difficult to design hard and superhard materials only on the basis of high stiffness.

4 Conclusion

In summary, we have used the first-principles calculations to systematically investigate the trends of stiffness and

hardness of Os, OsB, Os_2B_3, and OsB_2. The results indicate that Os possesses high stiffness but low hardness. Upon incorporating of boron atoms into Os to form OsB, Os_2B_3, and OsB_2, the hardness values of these borides enhance largely, although their stiffness decreases slightly. Such a crossover is a manifestation that the underlying sources of high stiffness and high hardness are fundamentally different. The stiffness is related to elastic deformation that is closely associated with valence electron density, whereas the hardness depends strongly on plastic deformation that is determined by bonding nature. Therefore, the incorporation of light atoms into transition metal should be a valid pathway of designing hard and superhard materials. This article not only clarifies the nature of some mechanical behaviors but also provides a useful strategy in the quest for intrinsically superhard transition-metal borides, carbides, and nitrides.

Acknowledgements: This work is supported by the National Natural Science Foundation of China (No. 51575398, 51072213), the State Oceanic Administration (No. SHME2013JS01), and the Science and Technology Commission of Shanghai Municipality (No. 13JC1402900, 14XD1424300).

References

[1] Y. Liang, J. Yang, X. Yuan, W. Qiu, Z. Zhong, et al., Sci. Rep. **4**, 5063 (2014).
[2] Y. Liang, Z. Wu, X. Yuan, W. Zhang, and P. Zhang, Nanoscale **8**, 1055 (2016).
[3] U. Lundin, L. Fast, L. Nordstrom, B. Johansson, J. M. Wills, et al., Phys. Rev. B **57**, 4979 (1998).
[4] J. Haines, J. M. Leger, and G. Bocquillon, Annu. Rev. Mater. Res. **31**, 1 (2001).
[5] R. F. Zhang, Z. J. Lin, Y. S. Zhao, and S. Veprek, Phys. Rev. B **83**, 092101 (2011).
[6] H. Cynn, J. E. Klepeis, C. S. Yoo, and D. A. Young, Phys. Rev. Lett. **88**, 135701 (2002).
[7] F. Occelli, D. L. Farber, J. Badro, C. M. Aracne, D. M. Teter, et al., Phys. Rev. Lett. 93, 095502 (2004).
[8] T. Kenichi, Phys. Rev. B 70, 012101 (2004).
[9] Y. Liang and B. Zhang, Phys. Rev. B **76**, 132101 (2007).
[10] R. B. Kaner, J. J. Gilman, and S. H. Tolbert, Science **308**, 1268 (2005).
[11] R. W. Cumberland, M. B. Weinberger, J. J. Gilman, S. M. Clark, S. H. Tolbert, et al., J. Am. Chem. Soc. **127**, 7264 (2005).
[12] H. Y. Chung, M. B. Weinberger, J. B. Levine, A. Kavner, J. M. Yang, et al., Science **316**, 436 (2007).
[13] L. Sun, Y. Gao, B. Xiao, Y. Li, and G. Wang, J. Alloy. Compd. **579**, 457 (2013).
[14] Y. Wang, T. Yao, L. M. Wang, J. Yao, H. Li, et al., Dalton Trans. **42**, 7041 (2013).
[15] Q. Li, D. Zhou, W. Zheng, Y. Ma, and C. Chen, Phys. Rev. Lett. **110**, 136403 (2013).
[16] B. Huang, Y. H. Duan, W. C. Hu, Y. Sun, and S. Chen, Ceram. Int. **41**, 6831 (2015).
[17] B. Huang, Y. H. Duan, Y. Sun, M. J. Peng, and S. Chen, J. Alloy. Compd. **635**, 213 (2015).
[18] Q. Gu, G. Krauss, and W. Steurer, Adv. Mater. **20**, 3620 (2008).
[19] Y. Liang, W. Guo, and Z. Fang, Acta Phys. Sin. **56**, 4847 (2007).
[20] Y. Liang, J. Zhao, and B. Zhang, Solid State Commun. **146**, 450 (2008).
[21] J. Yang, H. Sun, and C. Chen, J. Am. Chem. Soc. **130**, 7200 (2008).
[22] Y. Liang, A. Li, J. Zhao, and W. Zhang, Mod. Phys. Lett. B **23**, 1281 (2009).
[23] Z. W. Ji, C. H. Hu, D. H. Wang, Y. Zhong, J. Yang, et al., Acta Mater. **60**, 4208 (2012).
[24] J. P. Perdew, K. Burke, and M. Ernzerhof, Phys. Rev. Lett. **77**, 3865 (1996).
[25] G. Kresse and J. Furthmuller, Phys. Rev. B **54**, 11169 (1996).
[26] Y. Liang and Z. Fang, J. Phys.: Condens. Matter **18**, 8749 (2006).
[27] Y. Liang, B. Zhang, and J. Zhao, Phys. Rev. B **77**, 094126 (2008).
[28] Y. Liang, C. Li, W. Guo, and W. Zhang, Phys. Rev. B **79**, 024111 (2009).
[29] Y. Liang, W. Zhang, J. Zhao, and L. Chen, Phys. Rev. B **80,** 113401 (2009).
[30] R. Hill, Proc. Phys. Soc. **65**, 349 (1953).
[31] X. Q. Chen, H. Niu, D. Li, and Y. Li, Intermetallics **19**, 1275 (2011).
[32] Y. Liang, X. Yuan, and W. Zhang, Phys. Rev. B **83**, 220102(R) (2011).
[33] Y. Gou, Z. Fu, Y. Liang, Z. Zhong, and S. Wang, Solid State Commun. **187**, 28 (2014).
[34] Y. Liang, X. Yuan, Y. Gao, W. Zhang, and P. Zhang, Phys. Rev. Lett. **113**, 176401 (2014).
[35] Y. Liang, Z. Zhong, and W. Zhang, Comput. Mater. Sci. **68**, 222 (2013).
[36] F. Gao, J. He, E. Wu, S. Liu, D. Yu, et al., Phys. Rev. Lett. **91**, 015502 (2003).